

Supporting information: Structural characterization of model gels under preparation conditions and at swelling equilibrium

Reinhard Scholz, Michael Lang*

Leibniz Institute of Polymer Research Dresden, Hohe Straße 6, 01069 Dresden, Germany

<https://doi.org/10.1021/acs.macromol.3c02607>

I. FIT RESULTS FOR ξ AND Ξ

Table S1 summarizes the fit results for analyzing correlation lengths from the scattering data of the simulations. Data in italics have been excluded from fitting power law dependencies (see Table 1 of the main text) for the correlation lengths due to significant deviations from a power law relation. All of the excluded data lie either below c^* where the network structure becomes fluffy, or they refer to the highest concentration where a determination of ξ becomes difficult because of a small intensity decay over a narrow range of q vectors.

II. DATA AVERAGING

In a first step, star polymer solutions have been thermalized, and in a second step, selective bonds between A and B stars have been formed up to a conversion of $p = 0.95$. At this fixed conversion, independent frames are generated by choosing an adequate interval of Monte Carlo steps between consecutive frames. For the strand lengths of interest, relaxation times remain below 10^6 MCS, so that $X = 100$ frames in steps of 10^6 MCS between 1×10^8 MCS and 2×10^8 MCS are considered to be independent from each other. The scattering intensity for each frame is averaged over wave vectors with the same absolute value $q = |\mathbf{q}|$, and the data reported is averaged over all $X = 100$ frames. Since all data is given by discrete coordinates and not by smooth functions, we have to perform a discrete Fourier transform. As subsequent discrete values of q become very dense at large wave vectors, including all discrete q would require large numerical resources. Therefore, only for small q , Fourier transforms were calculated for all wave vectors with indices (j_x, j_y, j_z) according to eq. (1) of the main text, i.e. up to $\sqrt{j_x^2 + j_y^2 + j_z^2} \leq 16$, whereas each Cartesian component was sampled in steps of 2 in the surrounding shell of wave vectors with $16 < \sqrt{j_x^2 + j_y^2 + j_z^2} \leq 32$, in steps of 4 in the shell $32 < \sqrt{j_x^2 + j_y^2 + j_z^2} \leq 64$, etc. Moreover, on the basis of this discrete set of wave vectors, only for small q all values are included in the plots, whereas at

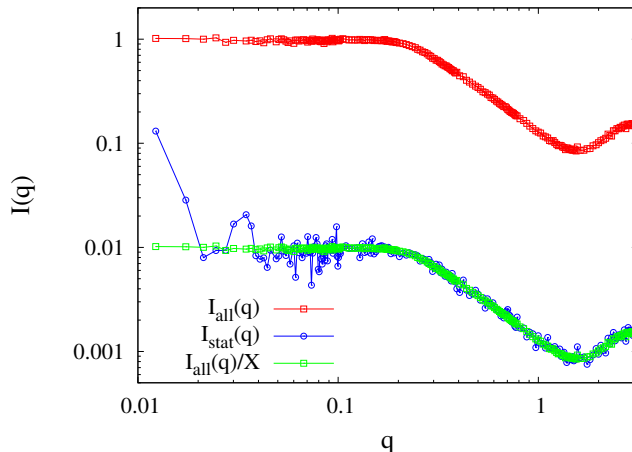


Figure S1: Comparison of total scattering data $I_{\text{all}}(q)$ and the corresponding static component $I_{\text{stat}}(q)$, for a solutions of stars with $N_A = 73$ and $N_B = 97$, prepared at a polymer volume fraction of $\phi_0 = 2\phi^*$.

larger q , the noise is reduced by reporting averages over 5 consecutive discrete values of q .

For splitting the scattering data into a static contribution $I_{\text{stat}}(q)$ and a dynamic contribution $I_{\text{dyn}}(q)$, care must be taken that the time interval between subsequent frames is sufficiently large to guarantee independence of the frames on the length scales of interest. Otherwise, the static contribution incorporates parts of an incompletely relaxed dynamic contribution in the low q limit that might lead to an incorrect data analysis. This can be tested with the data for the star polymer solutions: here, we expect that $I_{\text{stat}}(q) = I_{\text{all}}(q)/X$ for completely independent frames on all length scales, whereas $I_{\text{stat}}(q)$ becomes significantly (above the noise level of $I_{\text{stat}}(q)$) larger than $I_{\text{all}}(q)/X$ at length scales beyond which the frames are no more independent. Figure S1 shows that the frames are no more independent for a wave vector range $q < 0.02/u$. This observation is double checked by considering data on the relaxation time of linear chains. For $N = 82$ in melt, we expect from Ref [2] a relaxation time of the order of 10^6 MCS, which reduces to $\approx 10^5$ for the low ϕ_0 of our study due to the largely increased acceptance rate of the monomer moves. For our simulation model, the size of chains with $N = 82$ corresponds to wave vectors of about $q \approx 0.1/u$ [3], so that we expect a visible effect of incomplete averaging for $q \lesssim 0.03/u$. This agrees with the data in Figure S1. Incomplete averaging becomes relevant if the scattering intensity due to this effect becomes comparable with the scattering intensity of the static contribution of

* lang@ipfdd.de

N	M	ϕ_0	ξ_{sol}	ξ_{all}	ξ_0	Ξ_0	ϕ_1	ξ_{all}	ξ_0	Ξ_0	R_g	$\phi^{-1} = Q$	ξ_{all}	ξ	Ξ
23	51200	0.1373	1.532(9)	1.88(2)	1.53(2)	6.79(9)	0.142	1.33(3)	1.55(2)	6.6(1)	6.71	15.27	6.8(6)	4.364(7)	9.4(3)
	38400	0.1030	2.163(7)	2.80(2)	2.19(2)	7.58(7)	0.108	2.24(4)	2.227(7)	7.14(8)	6.84	16.66	7.7(7)	4.666(7)	10.0(3)
	25600	0.0687	3.179(5)	5.09(6)	3.433(6)	9.18(8)	0.074	4.34(7)	3.411(6)	9.0(1)	6.96	18.99	9.2(7)	5.81(2)	11.1(3)
	19200	0.0515	4.020(7)	7.7(2)	4.436(5)	10.55(9)	0.059	7.0(2)	4.610(7)	10.6(2)	7.01	20.92	10.8(9)	6.65(2)	12.2(4)
	12800	0.0343	5.42(1)	14.7(4)	6.17(2)	13.6(2)	0.044	13.1(3)	6.98(2)	13.7(2)	7.02	24.61	16(2)	8.93(3)	14.6(4)
	9600	0.0258	6.33(2)	25(1)	8.42(2)	16.8(2)	0.037	19.6(6)	9.30(3)	16.2(3)	7.00	27.82	20(2)	10.51(3)	16.5(4)
	6400	0.0172	7.64(2)	62(7)	13.94(4)	21.3(3)	0.028	32(2)	13.31(4)	20.2(3)	6.94	35.98	43(6)	15.60(5)	22.4(5)
43	38400	0.1945	0.94(1)	1.05(2)	0.939(9)	6.9(2)	0.198	1.03(1)	0.943(9)	6.7(2)	9.32	16.85	6.9(2)	4.126(6)	11.0(2)
	25600	0.1297	1.679(8)	1.89(2)	1.658(9)	8.0(2)	0.134	1.84(2)	1.63(1)	7.7(2)	9.70	20.40	7.9(5)	5.37(1)	11.9(4)
	19200	0.0973	2.325(7)	2.70(2)	2.292(9)	8.9(2)	0.102	2.69(2)	2.346(8)	8.8(2)	9.95	22.56	8.9(6)	6.04(2)	12.7(4)
	12800	0.0648	3.510(5)	4.52(5)	3.550(6)	10.9(2)	0.070	4.37(3)	3.541(7)	10.3(2)	10.21	25.72	10.9(7)	7.21(2)	14.1(4)
	9600	0.0486	4.541(5)	6.63(8)	4.593(7)	12.4(2)	0.054	6.42(5)	4.678(6)	12.0(2)	10.36	27.93	12.5(7)	8.01(2)	15.3(4)
	6400	0.0324	6.22(1)	12.2(3)	6.817(9)	15.7(2)	0.039	11.5(2)	6.87(2)	15.3(2)	10.48	32.17	16(1)	9.32(2)	17.7(4)
	3200	0.0162	10.22(2)	52(4)	12.10(3)	22.6(4)	0.025	35(2)	12.82(3)	21.3(3)	10.45	43.57	33(4)	14.40(4)	23.1(5)
82	12800	0.1244	1.769(9)	1.88(2)	1.71(1)	9.4(2)	0.128	1.86(1)	1.726(8)	9.3(2)	13.97	24.96	9.5(3)	6.09(2)	15.2(3)
	9600	0.0933	2.462(7)	2.71(2)	2.421(8)	10.9(3)	0.097	2.62(2)	2.450(7)	10.2(2)	14.33	29.45	11.4(5)	7.33(2)	17.0(4)
	6400	0.0622	3.812(6)	4.26(3)	3.700(7)	12.4(3)	0.067	4.16(3)	3.664(7)	11.9(3)	14.82	34.57	12.9(6)	8.70(2)	18.2(5)
	4800	0.0466	4.886(6)	6.02(4)	4.851(7)	14.5(2)	0.051	5.73(4)	4.863(6)	13.7(2)	15.10	37.95	15.2(8)	9.79(2)	19.7(5)
	3200	0.0311	7.24(2)	9.9(1)	7.04(2)	17.3(3)	0.036	9.26(8)	6.98(2)	16.5(2)	15.43	44.07	19.4(9)	11.54(3)	22.2(5)
	2400	0.0233	8.79(2)	15.2(3)	9.13(2)	20.1(3)	0.029	13.1(2)	8.69(2)	18.9(3)	15.55	47.04	20.6(9)	12.74(3)	23.0(5)
	1600	0.0155	11.91(2)	28.3(8)	12.72(3)	24.2(3)	0.022	24.1(5)	12.34(3)	23.5(3)	15.66	52.88	29(2)	15.27(3)	25.7(5)

Table S1: Left part: simulations with periodic boundary conditions (solution + networks), middle part: preparation state in non-periodic boundary conditions (networks), right part: equilibrium swelling in non-periodic boundary conditions (networks). Fit results for ξ_{sol} and ξ_{all} refer to a fit with equation (11) of the main text and $\nu = 0.5876$ to $I_{\text{all}}(q)$ of either a solution or of a network, at the corresponding effective polymer volume fraction ϕ_0 , ϕ_1 , or $\phi = 1/Q$. The dynamic correlation length ξ_0 and the static correlation length Ξ_0 were determined after splitting the data into $I_{\text{dyn}}(q)$ and $I_{\text{stat}}(q)$, see equation (27), Figure 3, and the discussion in the main text, including the exclusion of the region around the star hump for analyzing $I_{\text{dyn}}(q)$. Numbers in brackets define the error of the data fit, e.g. 9.4(3) refers to 9.4 ± 0.3 . Data for ϕ_0 , ϕ_1 , and Q was taken from preceding work [1]. The radius of gyration, R_g , was computed from the coordinates of the individual chains connecting two star centers, excluding the latter.

the network. This is clearly impossible for the samples at swelling equilibrium, see Figure 5 of the main text, since there $I_{\text{stat}}(q) \approx I_{\text{dyn}}(q)$ for low q . At preparation conditions, there is $I_{\text{stat}}(q) \ll I_{\text{dyn}}(q)$ for large ϕ_0 , however, this regime refers to the smallest Ξ , so that corrections due to an incomplete averaging do not interfere with a determination of Ξ .

III. THIN SLICES THROUGH SEVERAL NETWORKS AT PREPARATION CONDITIONS AND AT SWELLING EQUILIBRIUM

- [1] M. Lang, R. Scholz, L. Löser, C. Bunk, N. Fribicz, S. Seifert, F. Böhme, and K. Saalwächter, *Macromolecules* **55**, 5997 (2022).
[2] T. Kreer, J. Baschnagel, M. Müller, and K. Binder, *Macro-*

- molecules* **34**, 1105 (2001).
[3] M. Lang and R. Scholz, *Macromol. Rapid Commun.*, 202400025 (2024).

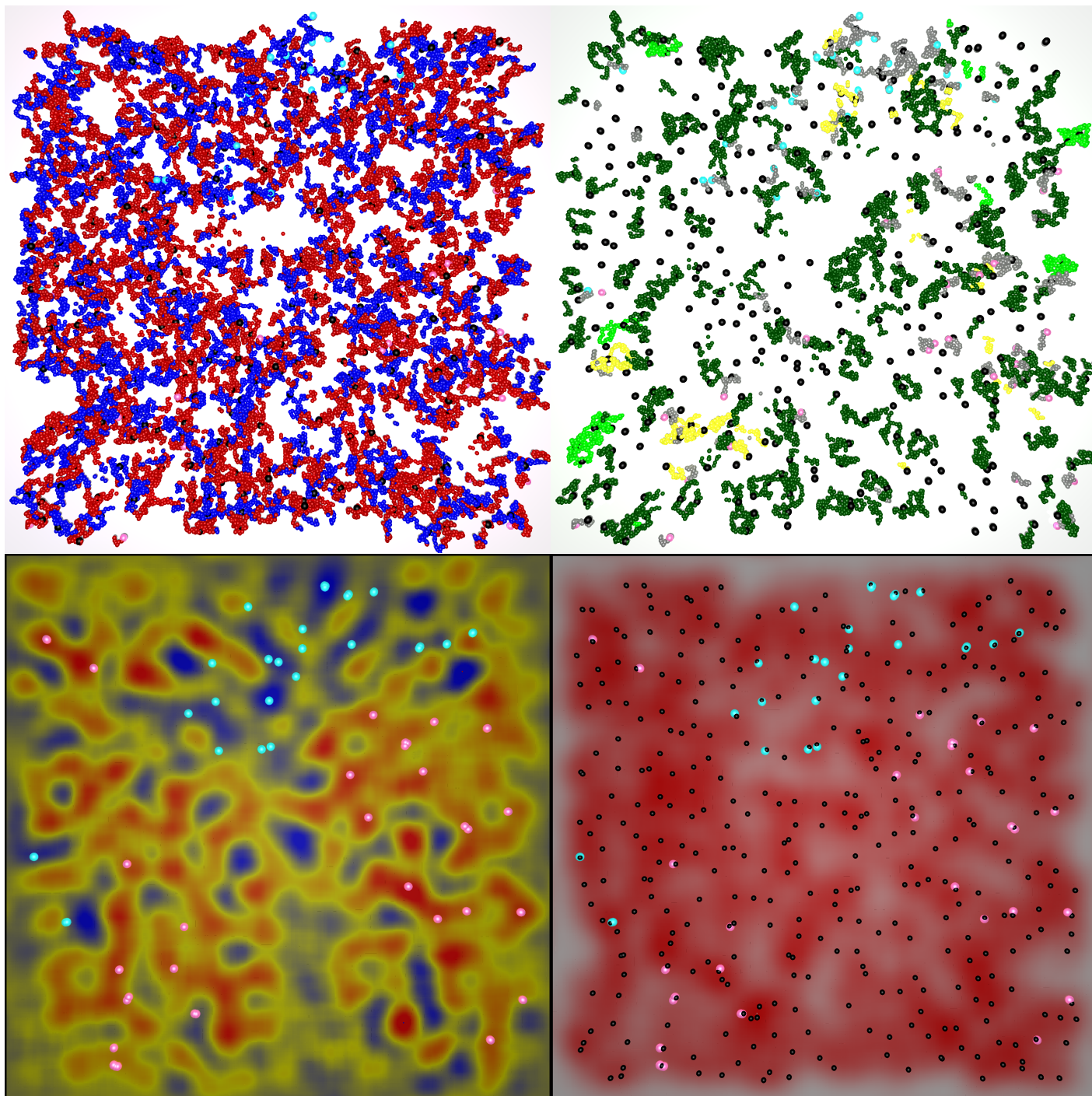


Figure S2: Thin slice with a thickness of 28 lattice layers, for the network with $N = 43$ prepared at ϕ^* in a box of 512^3 lattice sites. Top left: Snapshot - blue and red beads show A and B monomers, respectively, cyan and magenta are time average positions of non-reacted groups of A and B polymers, black beads are star centers. Top right: Defects and star centers (black beads) - double link (dark green), triple link (light green), extended strands (yellow; star centers inside these strands have only 2 connections to the network), pending material (gray - if not colored before), and sol (orange). Bottom left: time average density of A and B polymers on lattice are shown in blue and red, with domain boundaries in yellow. Bottom right: time average total density profile, star centers, and non-reacted ends of dangling arms.

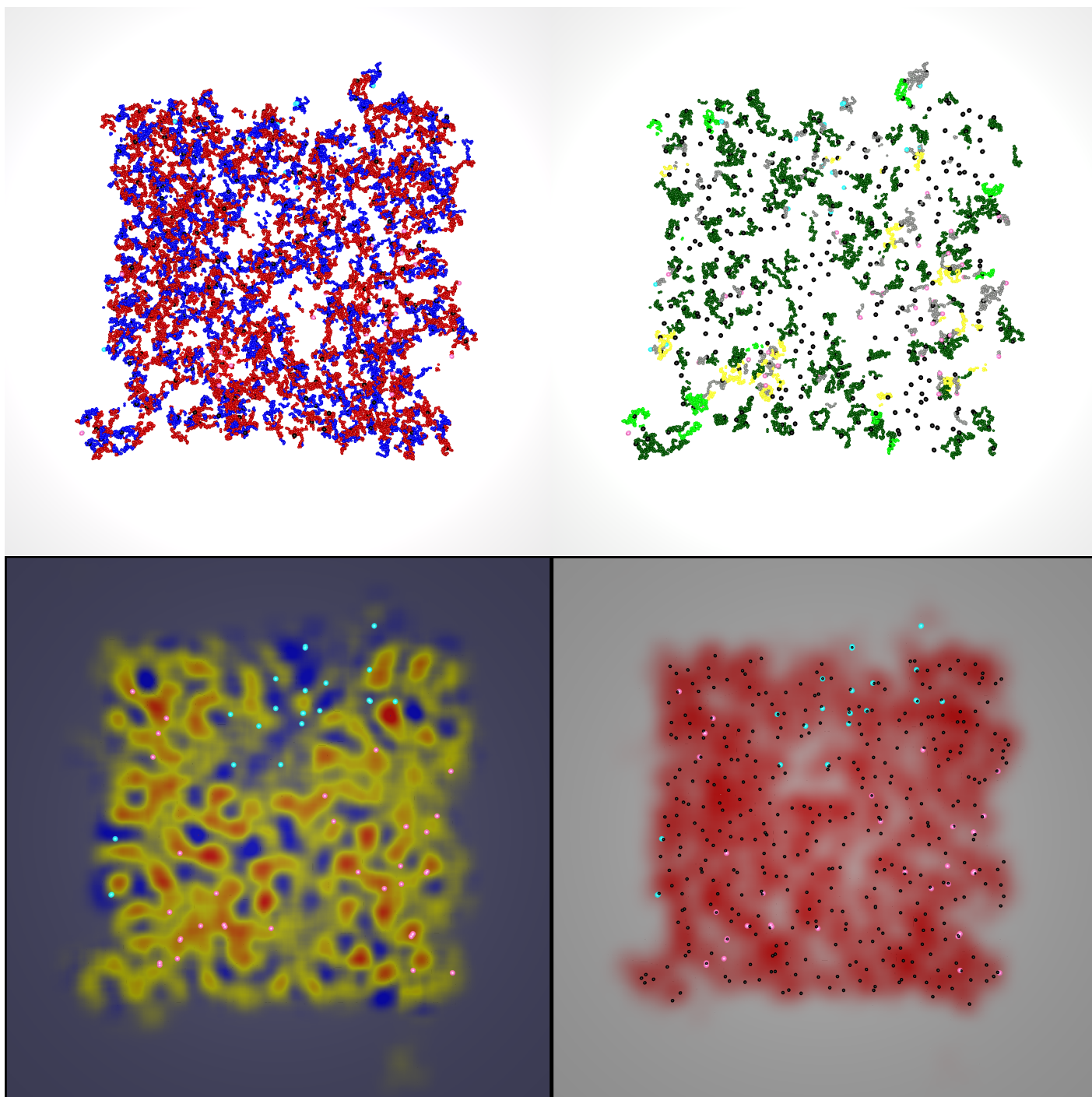


Figure S3: Swelling equilibrium of the same sample in a box of 800^3 lattice sites, at approximately the same location as in Figure S2, but now with a thickness of 32 lattice layers due to swelling. See Figure S2 for explanations.

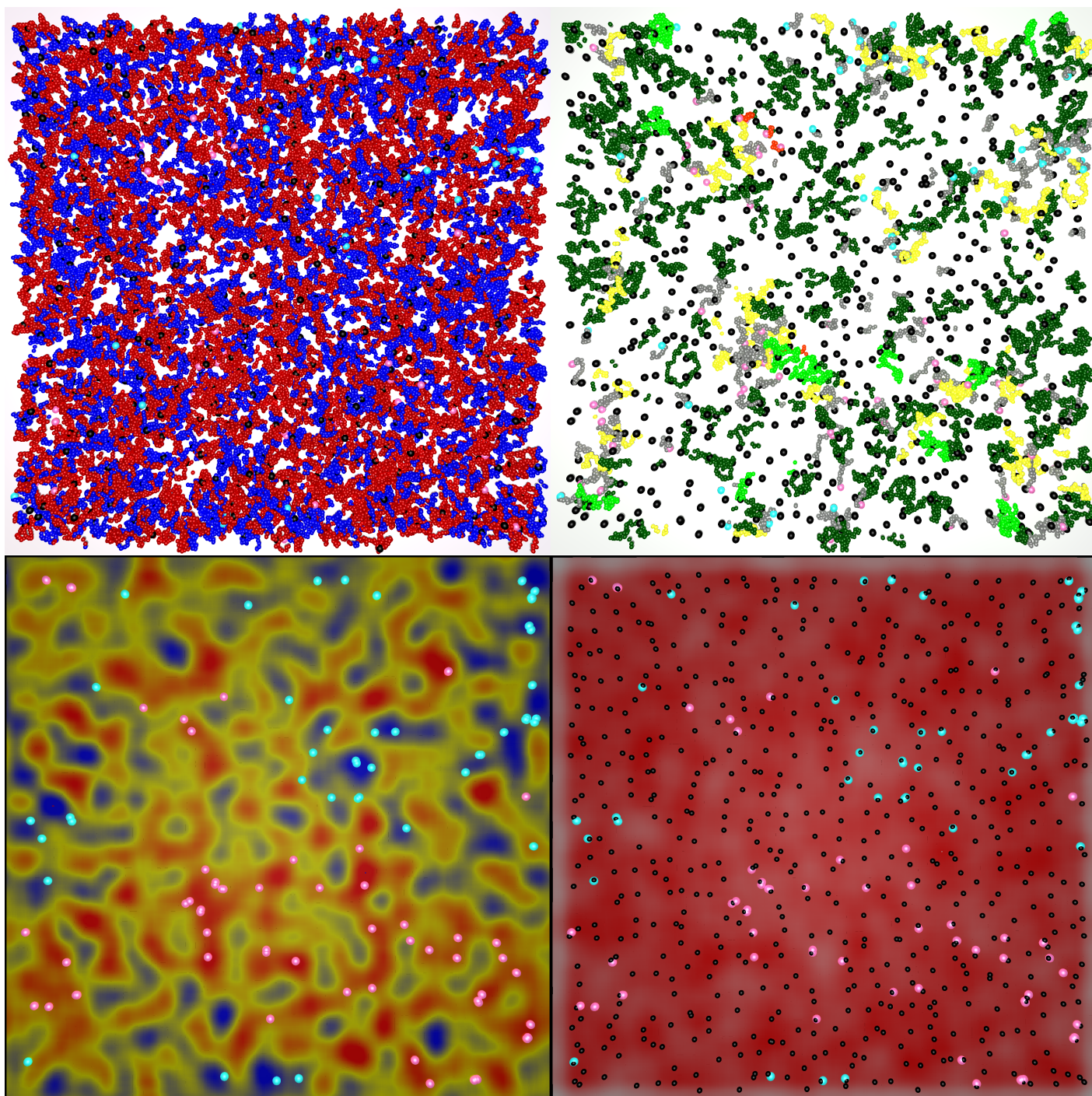


Figure S4: Thin slice with a thickness of 24 lattice layers, for the network with $N = 43$ prepared at $2\phi^*$ in a box of 512^3 lattice sites. Same analysis as in Figure S2.

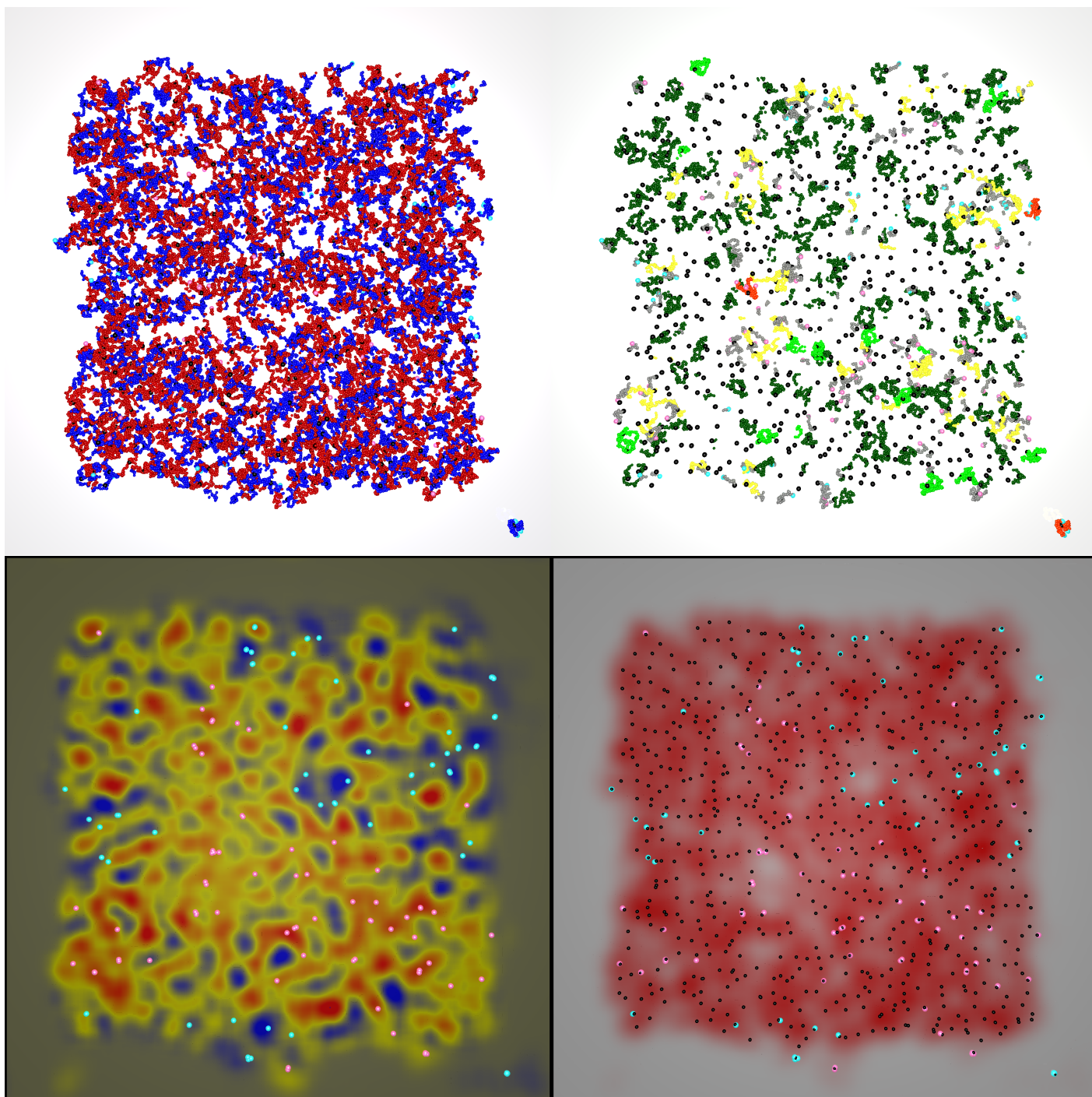


Figure S5: Swelling equilibrium of the same sample at approximately the same location as in Figure S4. Slices with a thickness of 32 lattice layers, see Figure S2 for explanations.

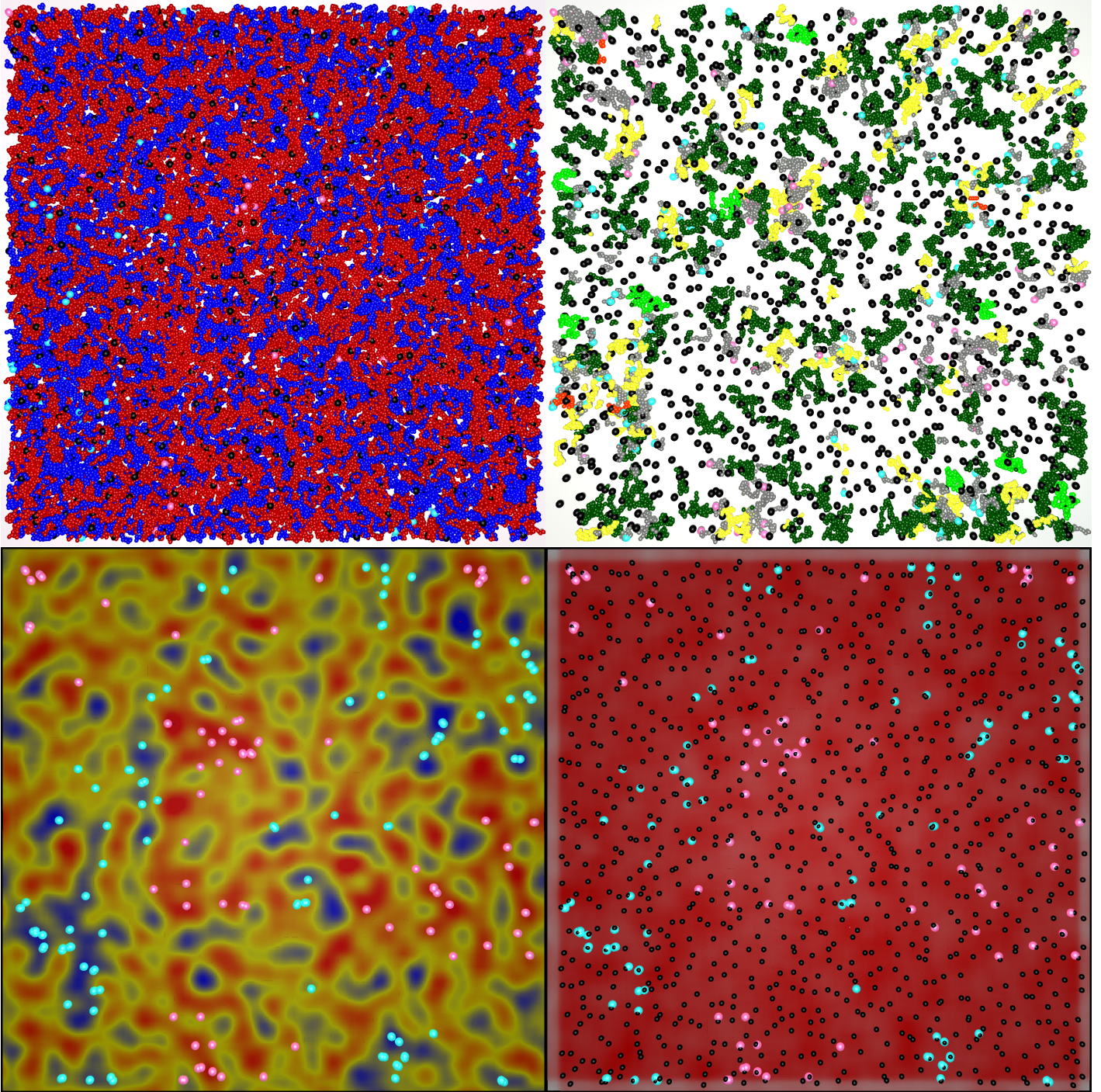


Figure S6: Thin slice with a thickness of 20 lattice layers, for the network with $N = 43$ prepared at $4\phi^*$ in a box of 512^3 lattice sites.

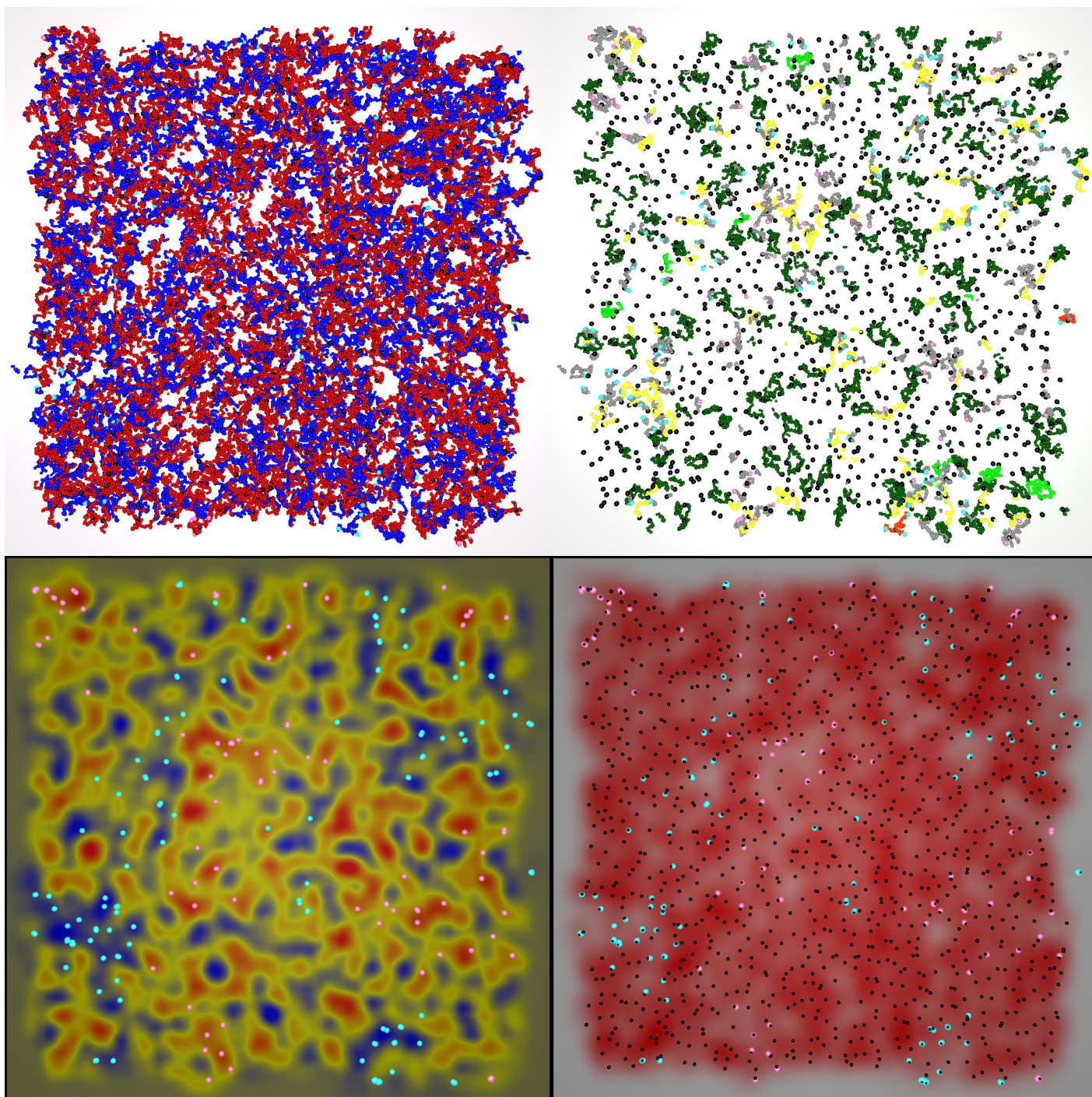


Figure S7: Swelling equilibrium of the same sample at approximately the same location as in Figure S6. Slices with a thickness of 32 lattice layers, see Figure S2 for explanations.